中國機械工程學刊第四十三卷第六期第 509~520 頁(民國一百一十一年)
Journal of the Chinese Society of Mechanical Engineers, Vol.43, No.5, pp.509~520 (2022)

Prediction of Transonic and Subsonic Wind Tunnel Aerodynamic Data by Neural Networks

Jun-Kai Ouyang*, **, Yi-Ting Liao*, Ying Li*** and Wei-Hsiang Wang****

Keywords: neural networks, wind tunnel, cavity flow, delta wing.

ABSTRACT

This study aims to build the backpropagation neural network model to predict wind tunnel aerodynamic data. The experiments were performed to obtain the pressure fluctuation on compressible cavity flows in transonic wind tunnel and used different sweep angle delta wing model to obtain the aerodynamic data in subsonic wind tunnel, respectively. The experiments data is used as the training parameter for neural network to decide the neural network structure, tuning the adjustable hidden layers and neuron number parameters of the neural network. The Levenberg–Marquardt (LM) technique is adopted as the weighting training algorithm to minimum the cost function. This article have established the neural network model to provide good agreement with experiments result. By using neural network technique, the wind tunnel test efficiency and aerodynamic data analysis can be significantly improved.

INTRODUCTION

Wind tunnel test has been a very important tools for the design of aircrafts, road vehicles and buildings. Depends on the velocity of flow fields and characteristics of aerodynamic forces, the subsonic, transonic and hypersonic wind tunnel facilities are adopted for different purpose to analyze the phenomena of the flow fields.

Paper Received March 2022. Revised October, 2022. Accepted October, 2022. Author for Correspondence: Wei-Hsiang Wang

* *Engineer, Department of Aerodynamics, Aeronautical Systems Research Division, National Chung-Shan Institute of Science and Technology, Taichung, Taiwan 407104, ROC.*

** *PhD Candidate, Department of Mechanical Engineering, National Chung-Hsing University, Taichung, Taiwan 40227, ROC.*

*** *Graduate Student, Department of Mechanical Engineering, National Chung-Hsing University, Taichung, Taiwan 40227, ROC.*

**** *Assistant Professor, Department of Mechanical Engineering, National Chung-Hsing University, Taichung, Taiwan 40227, ROC.*

Regarding the transonic flow, Krishnamuty (1955) studied the acoustic radiation emitted from two-dimensional rectangular cavity and observed strong acoustic energy is generated by the shear flow of the cavity. Rossiter (1964) used the shadowgraph technique to study the vortices over the cavity in the transonic wind tunnel, and developed a semi-empirical formula to predict the fluctuation frequency, then Heller et al. (1971) proposed a modified formula to extend the range of the free stream Mach number. Tracy and Plentovich (1993) measured the static and fluctuating pressure data of cavity flows. For supersonic and transonic cavity flow, they summarized four types of flow characteristics based on the ratio of cavity length and depth. In the case of $L/D < 10$, which is open type cavity flow, the air flow pass through the cavity and generate separation flow and free shear layer. This disturbance shear flow may propagate to downstream and form strong vortices and impinge the rear wall of the cavity, make the fluctuating pressure and acoustic waves move to upstream. Finally, this phenomenon becomes a feedback loop in the cavity and generates severe oscillating that makes the structure damage easily.

In general, aircraft designers use aerodynamic devices, such as strake, delta wing, canard and leading-edge extension, to generate strong vortices near the aircraft. These vortices not only produce extra life forces, but also make the aircraft more maneuverable due to the interaction of it. For example, the delta wing of Mirage-2000 may generate leading edge separation at high angle of attack with symmetrical pair of vortices (Gudmundsson, 2013). As a result, these vortices induce extra lift force to prevent the aircraft from stall condition at high angle of attack, and make it more flexible compared with conventional aircrafts.

Although the wind tunnel test can provide important information of aircraft design, the cost is usually very expensive and increased with the number of tests and execution time. In order to minimize the cost of experimental work, some numerical approaches and optimization of the measurement data are needed. In this study, we used neural network as a postprocessing tool to extend the usage of existing data by wind tunnel tests and predicted useful results of aerodynamic forces.

In recent years, neural networks have been widely used in various fields by simulating simplified biological neural network. In this study, the neural networks method is used to train and verify wind tunnel aerodynamic data. Generally, engineering problems are often difficult to describe and solve using a simple mathematical model due to the high-order nonlinearity terms in the governing equations. However, by using the learning and recall process of neural networks, the complex mathematical problems can be simplified through a series of learning, weight adjustment and training samples to obtain accurate solutions.

In this study, the wind tunnel test data is used as the training parameter in order to establish a suitable neural network model for aerodynamic analysis of cavity and delta wing models.

The concept of the neural networks is to imitate human or creature brain that all the artificial neurons are connected with each other to calculate and transmit signals. The earliest artificial neuron concept is proposed by McCullogh and Pitts (1943) which is just a simplistic mathematical model. Rosenblatt (1958) began to develop the original perceptron algorithm, and then Rumelhart (1986) proposed a multi-layer perceptron structure, this is the first neural network model which minimize the actual measure data and the desired output data by repeatedly adjusting weights.

Base on the connection method of neurons, there are varied neural network structures, which can be generally divided into feedforward neural networks and feedback neural networks. For feedforward neural networks, the neurons of the hidden layer are independent of each other, and the signal transmission is in one direction from input to the hidden layer. For the input layer, all parameters should be normalized or standardized first, and the excitation function, such as step function, unipolar S function or bipolar S function, is adopted for the hidden layer, which can be used as the same manner for output layer.

In contrast, the feedback connection is used between the hidden layer of the feedback type neural network, which means the output layer is connected back to the input layer, and the structure is more complicated than feedforward neural networks.

In practice, Neural network is widely used in many applications. Faller et al. (1994) developed a neural network model as a controller for prediction and controlled three-dimensional unsteady separated flow fields. Khan et al. (2021) adopted the feedforward neural network for predicting the efficiency of heat exchanger with different wing-width ratios. Efe et al. (2008) used the feedforward neural networks for subsonic shallow cavity flow control. Tabaza et al. (2021) used Levenberg–Marquardt algorithm to update the weighting and bias in the network. The results show that the prediction of the impact hysteresis problem between the ANN and experimental data is in good agreement.

The algorithm used in Neural network could be a key point that affects the accuracy and efficiency. Hagan and Menhaj (1994) used the LM method to integrate into the backpropagation algorithm, and used the neural network method to test the convergence of different waveforms. It was found that the MBP (Marquardt backpropagation) method had better convergence than the VLBP (Backpropagation with variable learning rate) and CGBP (Conjugate gradient backpropagation) methods. Cigizoglu et al. (2005) employed three different backpropagation algorithms, Levenberg–Marquardt, conjugate gradient and gradient descent for predicting performance and convergence velocity. It was shown that the feedforward backpropagation method with Levenberg–Marquardt technique provided shorter training duration and more acceptable performance criteria advantages compared with feedforward backpropagation with gradient descent technique and conjugate gradient.

Yanis et al. (2021) used the artificial neural networks method to predict the surface roughness of the AISI 1045 material by side milling process. The results of the analysis show that the best BP algorithm in predicting experimental data is LM method.

Hoyos et al. (2022) combined the Levenberg-Marquardt algorithm and particle swarm algorithm to construct a feed-forward neural network as a fast tool to predict the small size propellers, and the neural network model is trained with a large set of experimental data to predict the propeller performance coefficients.

In this paper, we discussed the aerodynamic characteristic of the cavity and delta wing model in the wind tunnel test and used measure data as the training parameter for neural network. The trained neural network model can be used to predict the pressure of the cavity at specific position and obtain the delta wing lift/drag coefficient.

EXPERIMENTAL SETUP

The transonic test is conducted at NCSIST/ASRD by a blow down and open circuit type wind tunnel. The test section is 120 × 120 cm^2 and 150 cm in length, and the operation Mach number is from Mach number 0.4 to 4.5 which cover supersonic, transonic and subsonic region. The compressed air used in the wind tunnel is stored in the four storage tanks. The capacity of four storage tanks is 1415.8 m^3. The compressed air flows out of the storage tanks through the ball valve and sleeve valve to obtain the stagnation pressure, and then through the stilling chamber where honeycomb and screen are installed to improve the uniformity of the flow.

After that, air flows through the convergent-divergent nozzle section to accelerate and flow into the test section. The transonic test section is used when the operation condition is from Mach number 0.4 to 1.4. The transonic test section is assembled with perforated walls, and at the end of the test section, the Mach flap and choke flap devices are used to control the flow speed under transonic range.

The test model is a flat plate with an acute angle of 6° leading edge , and the outer dimensions are 645 mm × 147 mm × 25 mm (length × width × thickness) in the transonic wind tunnel test, and the cavity size is in rectangular shape with 90 mm × 42.9 mm × 15 mm (length × width × depth). The length-to-depth ratio (L/D) is 6 and can be treated as an open type cavity as shown in Figure 1. The supported base of the model is installed on the side wall of the wind tunnel. When the air flows through the flat plate. A turbulent boundary layer is then developed naturally on the plate.

Position of pressure sensors in the rectangular cavity model are shown in Figure 2. The pressure data of K3/K5/K7/K9 are as input parameters and K8 as output parameters for training neural network model.

The flow condition in transonic wind tunnel defined by Mach number are 0.6, 0.7, 0.8, 0.85, 0.9, 0.95, 1.05 and 1.2±0.01 with the Reynolds number of 1.92×10^{6} and the stagnation pressure P_0 is varied from 23 to 30 psi (137 to 206 kpa), the stagnation temperature T_0 is varied from 25 to 35°C. The boundary layer thickness (δ) measured in front of the cavity model at X= -46mm is approximately 7.6mm.

In contrast, the delta wing model is conducted by the subsonic wind tunnel at NCSIST/ASRD, which is a horizontal, close-circuit type tunnel. The wind tunnel test section size is 3230 mm in width and 2280 mm in height. The power system of the subsonic wind tunnel is a 1500 horse power motor with 7-blade, pitch-fixed propeller. The maximum Mach number is 0.25, corresponding to 320 km/h. The angle of attack of the model support system is from -90° to 90° and the sideslip angle is from -22.5° to 22.5°.

Fig. 1. Cavity model installed in transonic wind tunnel

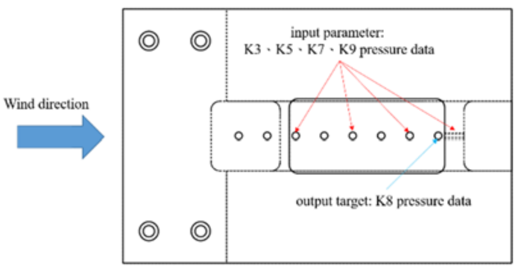

Fig. 2. Position of pressure sensors in the rectangular cavity model

The delta wing model is configured with three different sweep angles in the subsonic wind tunnel to obtain the characteristics of aerodynamic forces and to verify with the neural network results. The total length of the model is 847.75 mm with a fuselage diameter of 77.47 mm, and wing sweep angles are 45°, 57° and 63°, repectively. The model is made by 7075-T651 aluminum alloy and the internal balance bushing of the model is made of 17-4 stainless steel, and a six-component balance is installed in it. The delta wing test model is shown in Figure 3, a straight support from the end of the model is used to connect the wind tunnel support system which can provide -5°~30° angle of attack. The Mach number is set to 0.2, and the Reynolds number is 0.488×10^{6}**.** The sweep angles and angle of attack are chosen as input parameters and measure dlift/drag coefficients as output parameters.

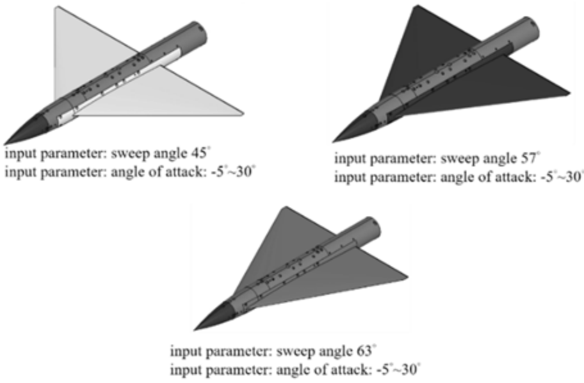

Fig 3. Different sweep angle delta wing models

The control and data acquisition system of the transonic wind tunnel produced by National Instruments (NI) was used during the test. The system is equipped with PXI acquisition cards, FPGA cards, digital output/input interface cards, etc. To control the wind tunnel system and capture system status such as temperature, stagnation pressure, potentiometer position and distance, etc. The dynamic pressure signal acquisition for the cavity model is by the DEWETRON dynamic data acquisition instrument (model: DEWE2-A13) and the data sampling rate is set to 5μs, and the 60 kHz low-pass filter is adopted for data filtering.

The dynamic pressure sensor used in the test is Kulite XCS-190-25A and powered by DEWETRON dynamic data acquisition instrument of DC 12V, the Kulite diameter of the pressure sensing part is 3.8mm, and the natural frequency is 200 kHz. The signal is sent to the dynamic data acquisition device to convert the voltage into pressure data by calibration slope, and the maximum error is 0.5% of the full scale operation range.

Besides, the subsonic wind tunnel control and data acquisition system are produced by HP VXI Instruments. The six-component internal balance is used to measure the static force and moment in the subsonic wind tunnel of the delta wing model. Based on the calibration results, the maximum error of each component is less than 0.5% maximum force load.

NEURAL NETWORK METHODOLOGY

The structure of back propagation neural network used in this study is a kind of multi-layer perceptron network. The training data is feed forward while the error propagates backward. Since the supervised learning model is adopted, each set of training data for input comes with a corresponding output data for comparison.

For transonic cavity case, the training data used is the pressure data measured at positions K3, K5, K7 and K9, and the Mach number is considered as well. Therefore, a total number of five training data set is used. The measured results of position K8 are compared with the output layer of neural network for parameter tuning process.

On the other hand for the subsonic delta wing test, the sweep angle of delta wing and the angle of attack are selected as input training data where the lift and drag coefficients are the output data.

During the training process, the weighting factors in the scheme are adjusted to minimize the difference between the target values and the training results, and the target function E is calculated by,

$$E(\omega) = \frac{1}{2}\sum(T_i - y_i)^2 \tag{1}$$

where T is the ith target value, y is the ith training output.

Conventionally, the determine of weighting factor of the backpropagation neural network is by the gradient descent method. In order to minimize the target function, the weight ω is updated as follows:

$$\nabla E(\omega_k) = -\eta\frac{\partial E}{\partial\omega} = \mathrm{J}(\omega_k)^T E(\omega_k) \tag{2}$$

where η is the learning rate, $\nabla E(\omega_k)$ is the gradient of target function, $J(\omega_k)$ is the Jacobian matrix.When using the gradient descent method for training, the converged speed is good at beginning but worth near the convergence point since the gradient become smaller while the characteristic of Newton's method is opposite. In order to solve this issue, the Levenberg-Marquardt algorithm is adopted in this study to update the weighting value and ω can be updated by the following relation:

$$\omega_{k+1} = \omega_k - (\mathrm{J}(\omega_k)^T\mathrm{J}(\omega_k) + \mu I_{N\times N})^{-1}\mathrm{J}(\omega_k)^T E(\omega_k) \tag{3}$$

where $k=1...N$, I is the identity matrix. For small μ, the characteristic of Newton's method dominates the algorithm while for large μ, it is similar to the gradient descent method of the backpropagation. Therefore, the Levenberg-Marquardt algorithm has the advantages of these two methods by changing the convergence method in the area where it is difficult to converge, and enhance the applicability of the neural network.

RESULTS AND DISCUSSIONS

The structure of the neural network in this study consists of three layers, the input layer, the hidden layer, and the output layer. Since the number of hidden layers and the arrangement of neurons will affect the learning rate and accuracy of the neural network, they are determined mostly by trail and tuning process. In this study, the structure of neural network is adopted by one input layer, one hidden layer with four neurons, and one output layer as shown in Figure 4. For the transonic test, the output value is the pressure value measured by the dynamic pressure sensor at K8 position on the cavity bottom plate, while for the delta wing case, the output value are lift and drag coefficient.

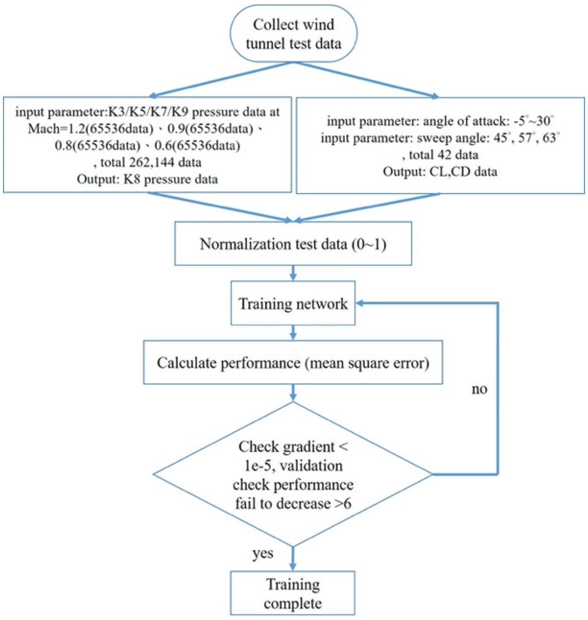

Fig. 4. The diagram of the neural network model

All the data are represented by 70 % for training, 15% for validation, and 15% for testing. The batch size is five for cavity training and two for delta wing training.

The sigmoid transfer function is used in the hidden layer, and the linear transfer function is for the output layer. The mean square error is 0.00181 for cavity model case after 96 epoch training and 0.000118 for delta wing model case after 25 epoch training to converge, as shown in Figure 5.

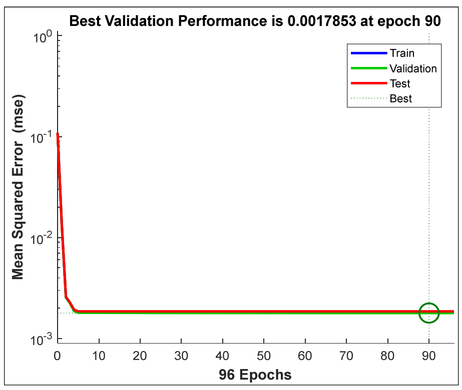

(a)Training result for cavity case

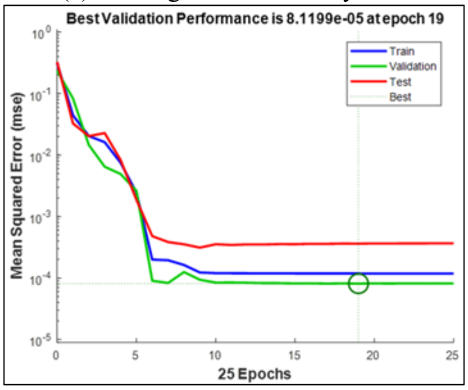

(b)Training result for delta wing case

Fig. 5. Training result of neural network model

The Cavity Pressure Measurement and Neural Network Training Result Comparison

In the cavity model case, four different Mach number (0.6, 0.8, 0.9 and 1.2) are trained, and each measurement location for each Mach number provides 65536 pressure data, and the total number are 262144 data per location. The pressure measurement data error calculation is as follows:

$$RMSE\ Error = \sqrt{\sum(T_i - y_i)^2/\mathrm{n})} \qquad (4)$$

where n is the number of data, the difference between the training results and the experiment results of the pressure measurement data at the cavity position K8 is shown in Figure 6.

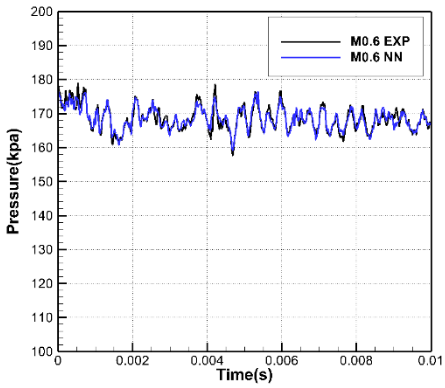

(a)Mach 0.6 (MSE=1.589kpa)

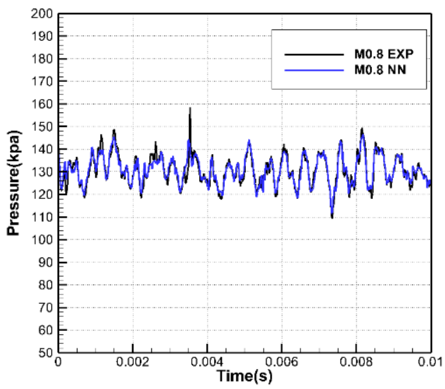

(b)Mach 0.8 (MSE=2.049kpa)

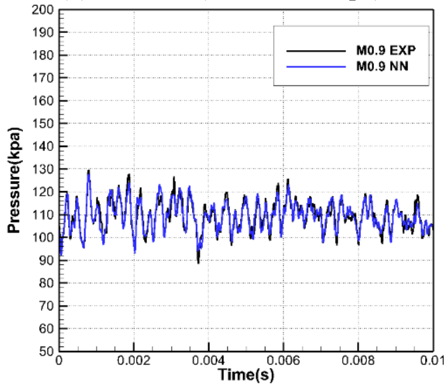

(c)Mach 0.9 (MSE=2.516kpa)

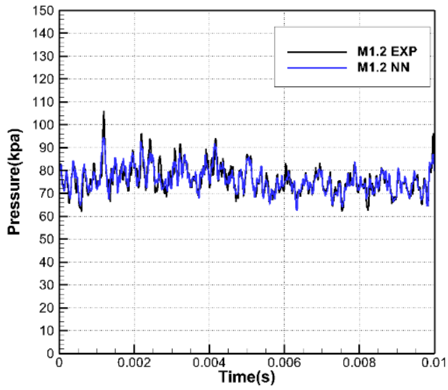

(d)Mach 1.2 (MSE=2.498kpa)

Fig. 6. Comparison of experiment and neural network result in time history at different Mach number.

According to the neural network training results, untrained pressure data of K3, K5, K7, K9 of Mach number 1.05, 0.95, 0.85, 0.7 are used as input parameters to predict the pressure data of the cavity K8 position, as shown in Figure 7.

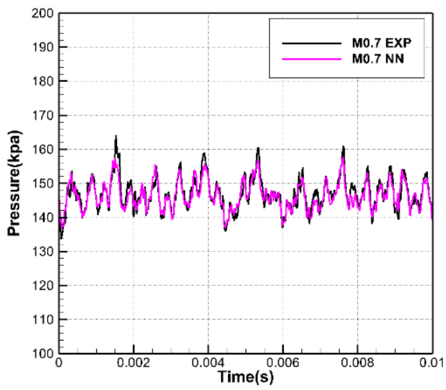

(a)Mach 0.7 (MSE=1.948kpa)

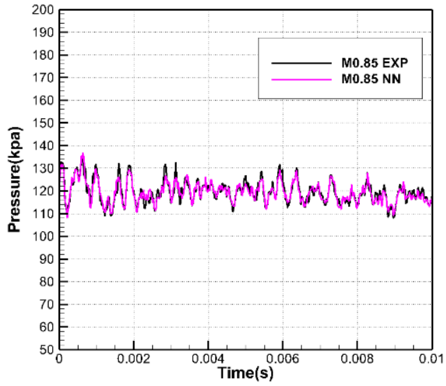

(b)Mach 0.85 (MSE=2.190kpa)

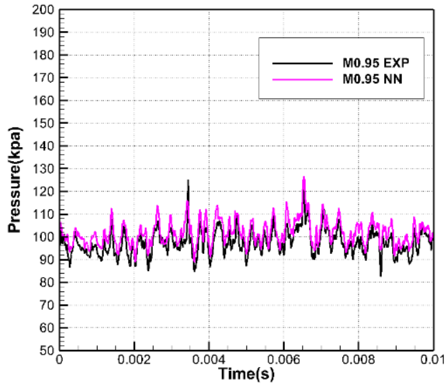

(c)Mach 0.95 (MSE=4.823kpa)

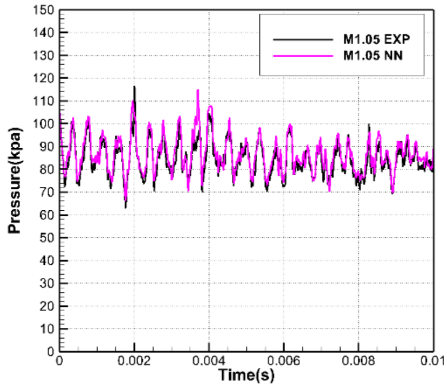

(d)Mach 1.05 (MSE=3.440kpa)

Fig. 7. New input parameter for comparison of experiment and neural network result in time history at different Mach number

The comparison of MSE error between experiments and neural network results of each Mach number are shown in Table 1. It is suggested that by using the training neural network model, the pressure results can be reasonably predicted.

Table 1. Pressure comparison between measurement and neural network at different Mach number

Training Mach number	MSE (kpa)	Untrained Mach number	MSE (kpa)
1.2	2.498	1.05	3.440
0.9	2.516	0.95	4.823
0.8	2.049	0.85	2.190
0.6	1.589	0.7	1.948

In addition to the pressure data in time domain, the results in frequency domain is considered as well in this study. Because of the airflow that passing through the cavity and generating periodic vortices in it, strong oscillations inside the cavity are induced with broadband frequencies. Through the Fast Fourier transform (FFT), the oscillation frequency can be understood quantitatively. Therefore, the pressure data at K8 is than converted into the frequency domain by FFT and be expressed as sound pressure level (SPL) which is calculated as follows:

$$SPL(dB) = 20\log10\frac{\mathrm{P}_{rms}}{\mathrm{P}_{ref}} \quad (5)$$

where P_{rms} is the root mean square of pressure, and P_{ref} is the reference sound pressure ($P_{ref} = 2 \times 10^{-5}\, pa$). The relationship between frequency and SPL is shown in Figure 8. It is shown that the training and verification results of the neural network model by FFT are consistent with the experimental spectrum results. It can be observed that for the cavity used in this study, which is L/D=6, the SPL of peak frequencies are over 150dB. This is due to the strong oscillations caused by the interaction of compressible flow and the cavity geometry.

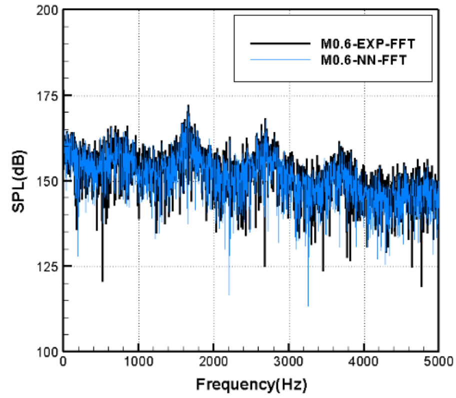

(a)SPL spectrum at Mach 0.6

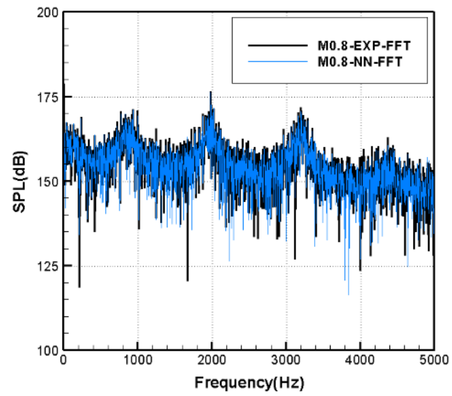

(b)SPL spectrum at Mach 0.8

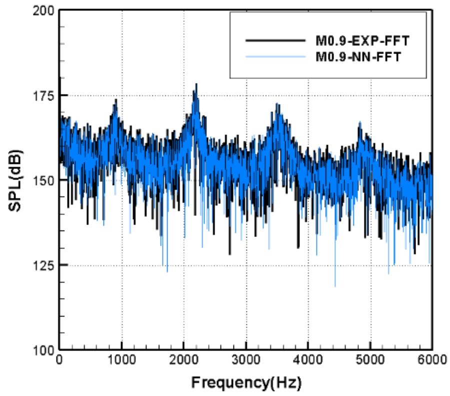

(c)SPL spectrum at Mach 0.9

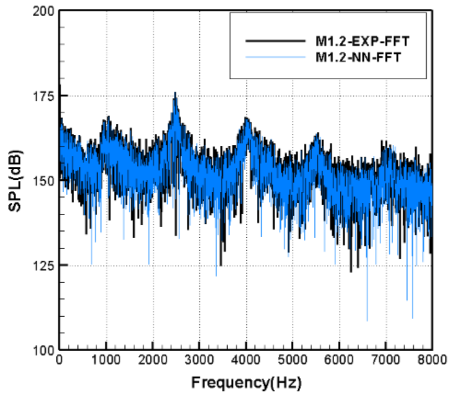

(d)SPL spectrum at Mach 1.2

Fig. 8. Position K8 SPL spectrum comparison of experiment and neural network result at different Mach number.

In order to analyze the relation between the neural network training results, experimental data and theory results, the semi-empirical formula for cavity modal prediction developed by Rossiter is used:

$$St = \frac{fL}{U} = \frac{m-\alpha}{M+\frac{1}{k}} \tag{6}$$

$$f = \frac{U}{L}\frac{(m-\alpha)}{(M+\frac{1}{k})} \tag{7}$$

And corrected by Heller for the semi-empirical formula:

$$f = \frac{U(m-\alpha)}{L\left[\frac{1}{k}+\frac{M}{\sqrt{1+0.5(\gamma-1)M^2}}\right]} \tag{8}$$

where U is the free flow velocity, m represents the mode number, γ is the specific heat, k and α are semi-empirical formula constants (k=0.57, α=0.25, and the available Mach number range is Mach number 0.4~1.12), L is cavity length (L=0.09m).

By comparing the results of the neural network with the experimental data and semi-empirical formula results, as shown in Table 2 and Figure 9. It is shown that the neural network training results or the experimental results are well consistent with the semi-empirical formula prediction results, which suggests that the neural network can provide reasonable prediction for the local transient pressure data and spectrum of the cavity flow.

Table 2. Modal frequency results of the cavity between the neural network result, the experimental results and the semi-empirical formula result

Mach number	Mode	NN result(Hz)	exp result(Hz)	semi-empirical formula(Hz)
0.6	Mode 1	830	720	728
0.6	Mode 2	1660	1672	1700
0.6	Mode 3	2686	2698	2671
0.6	Mode 4	3711	3674	3642
0.7	Mode 1	732	744	819
0.7	Mode 2	1868	1868	1910
0.7	Mode 3	2991	2991	3002
0.7	Mode 4	3979	3979	4094
0.8	Mode 1	842	842	904
0.8	Mode 2	1990	1990	2109
0.8	Mode 3	3162	3210	3314
0.8	Mode 4	4382	4382	4520
0.85	Mode 1	793	805	945
0.85	Mode 2	2100	2075	2205
0.85	Mode 3	3369	3369	3464
0.85	Mode 4	4602	4688	4724
Mach number	Mode	NN result(Hz)	exp result(Hz)	semi-empirical formula(Hz)
0.9	Mode 1	915	915	985
0.9	Mode 2	2197	2197	2298
0.9	Mode 3	3491	3491	3611
0.9	Mode 4	4834	4834	4924
0.95	Mode 1	939	939	1024
0.95	Mode 2	2307	2246	2389
0.95	Mode 3	3699	3699	3754
0.95	Mode 4	5066	5066	5120
1.05	Mode 1	964	964	1100
1.05	Mode 2	2429	2429	2566
1.05	Mode 3	3857	3857	4033
1.05	Mode 4	5359	5359	5499
1.2	Mode 1	1050	1038	1209
1.2	Mode 2	2478	2478	2821
1.2	Mode 3	4041	4041	4434
1.2	Mode 4	5542	5542	6046

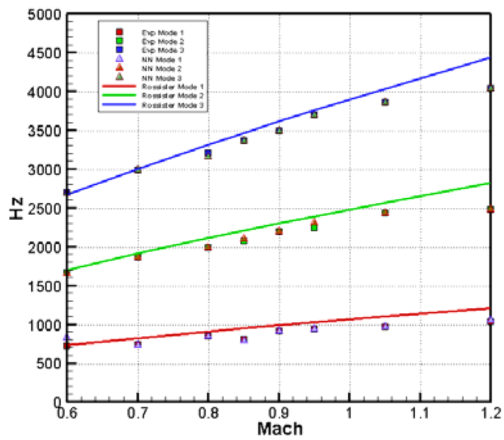

Fig. 9. Comparison of the neural network with the experimental results and semi-empirical formula result

Comparison results of lift-drag coefficients of delta wing in low-speed wind tunnel

In this study, based on the aerodynamic data obtained from the wind tunnel test, a backpropagation neural network model was established. The delta wing sweep angle and attack angle are used as training parameters for input layer where the output layer are lift coefficient and drag coefficient of the delta wing. Figure 10 shows the comparison of lift/drag coefficient with different angle of attack between the experimental results of three different sweep angle delta wings and the training results of the neural network, and the comparison are shown in Table 3. It is found that the training results of the neural network in this study are well consistent with the experimental results.

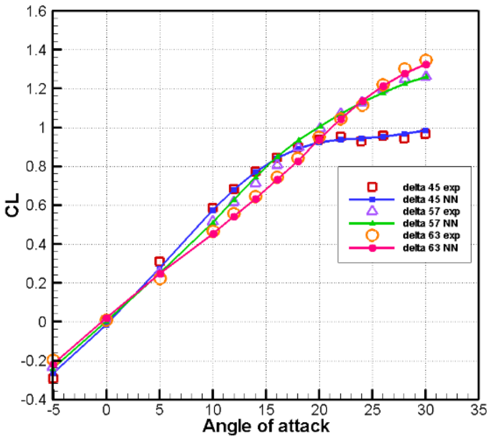

(a)Lift coefficient of different sweep delta wing

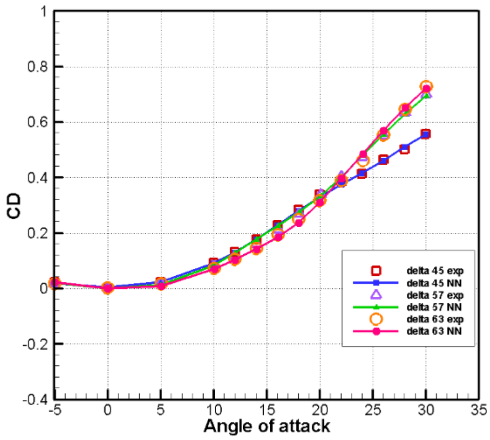

(b)Drag coefficient of different sweep delta wing

Fig. 10. Comparison of the neural network and the experimental results

Table 3. Lift and drag coefficient of the neural network and the experimental results

sweep 45˚				
angle of attack(˚)	experimental CL	experimental CD	neural network CL	neural network CD
-5.04	-0.2929	0.023	-0.2653	0.0176
-0.02	0.0094	0.0018	-0.0161	0.0043
4.98	0.3102	0.0227	0.2746	0.0229
9.99	0.5853	0.0917	0.5746	0.0898
11.97	0.6823	0.1315	0.6788	0.1294
13.99	0.7715	0.1776	0.7688	0.1764
16.01	0.843	0.228	0.8402	0.2281
17.98	0.9006	0.2837	0.8907	0.2796
19.99	0.9374	0.3383	0.922	0.3288
22.03	0.9509	0.3834	0.936	0.3733
23.96	0.9297	0.4129	0.9424	0.4143
26	0.9566	0.4648	0.9523	0.461
27.98	0.944	0.5006	0.9668	0.5088
29.99	0.9663	0.5558	0.9836	0.5553
sweep 57˚				
angle of attack(˚)	experimental CL	experimental CD	neural network CL	neural network CD
-5.07	-0.2345	0.0192	-0.2417	0.0212
-0.04	0.0096	0.0017	0.0012	-0.0004
4.98	0.2516	0.019	0.2467	0.0122
9.97	0.5132	0.0793	0.5077	0.0827
11.99	0.6131	0.1166	0.6262	0.1273
13.99	0.7111	0.1599	0.7429	0.1763
16.03	0.8046	0.2107	0.8489	0.2265
18.04	0.8972	0.2684	0.9341	0.2762
20.07	0.9944	0.3366	1.006	0.3337
22.01	1.0687	0.4023	1.0686	0.4001
24.03	1.1266	0.4722	1.1285	0.4777
25.99	1.1945	0.5504	1.1794	0.554
28.04	1.2471	0.6327	1.2239	0.6288
30.05	1.259	0.6987	1.259	0.6934
sweep 63˚				
angle of attack(˚)	experimental CL	experimental CD	neural network CL	neural network CD
-5.01	-0.1992	0.0167	-0.2177	0.0226
-0.04	0.0075	0.0016	0.0194	-0.0008
5.05	0.2225	0.0171	0.2477	0.0082
10.02	0.4639	0.0724	0.4531	0.0688
11.99	0.5545	0.1045	0.54	0.1036
14.01	0.6443	0.1442	0.6322	0.1414
16.08	0.7441	0.1938	0.7304	0.1848
17.97	0.8411	0.2482	0.8269	0.2363
20	0.948	0.3163	0.9369	0.3092
22.03	1.0423	0.3886	1.0442	0.3955
24.04	1.1131	0.461	1.1383	0.4854
25.99	1.2192	0.553	1.2141	0.5699
28.03	1.3014	0.6454	1.277	0.6506
30.05	1.3448	0.7271	1.3247	0.72

From the results of the lift coefficient, it is found that the lift coefficients of the sweep angles 57˚ and 63˚ are significantly higher than the sweep angle 45˚ when angle of attack is higher than 20˚. Figure 11 reveals the visualization of flow fields corresponding to the aerodynamic characteristic mentioned above. Apparently, the vortex breakdown occurs on the surface of the leading edge of the delta wing at sweep angle 45˚ when the angle of attack reached 22˚, which causes the wing stall. However, it is not occurred in sweep angles 57˚ and 63˚ delta wing even the angle of attack reached 24˚. The larger sweep angle can produce more lift to postpone the stall angle.

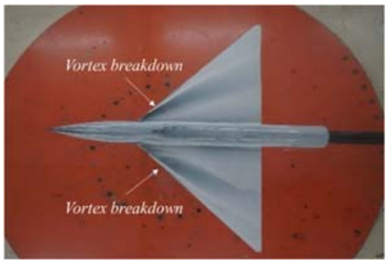

(a)sweep angle 45˚ delta wing (angle of attack=22˚)

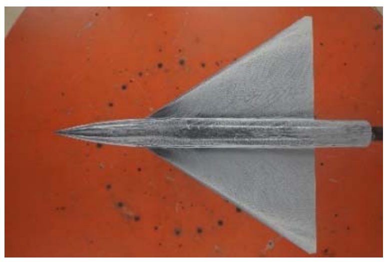

(b)sweep angle 57˚ delta wing (angle of attack=24˚)

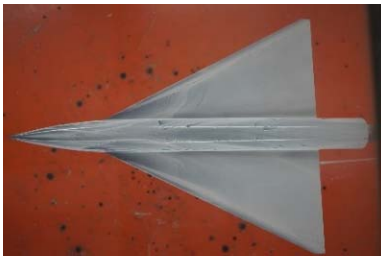

(c)sweep angle 63° delta wing (angle of attack=24°)

Fig. 11. Flow visualization of delta wing

Since the training of neural network is finished, we changed the sweep angles (50°, 60°, and 65°) as new input parameters, and obtained the prediction lift coefficient and drag coefficient by the model. The results are shown in Figure 12, and it is observed that the aerodynamic characteristic of the sweep angle 50° is similar to sweep angle 45°,that the stall angle of attack is about 20°. Besides, the sweep angles of 60° and 65° have the characteristics that keeping the high lift force under higher angles of attack, which is similar to the experimental results of 63° sweep angle. Furthermore, by comparing the sweep angle of 50°, 60°, 65° lift/drag coefficient with Verhaagen (2012), Rinoie (2000), Al-Garni (2008) which are shown in Figure 13 to Figure 17, mostly the results of neural network prediction are well consistent with the experimental results. The only difference in Figure 13 is that when the angle of attack is larger than 20°, the stall is observed in the experimental data which is not shown in the present study. However, it is due to the different configurations of the delta wing between these two cases. For present study, the delta wing is connected to the aircraft body, but for Verhaagen (2012), it is performed by wing itself, which makes the difference.

To summarize, from the results mentioned above, it is clear that the application of neural network method to the aerodynamic prediction with different sweep angle of delta wing can provide reasonable and accurate information.

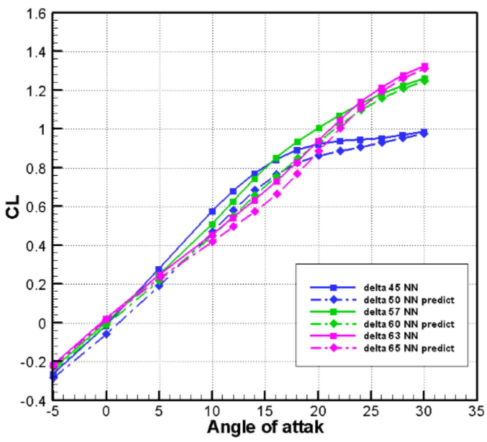

(a)Lift coefficient prediction for 50°, 60° and 65° sweep delta wing

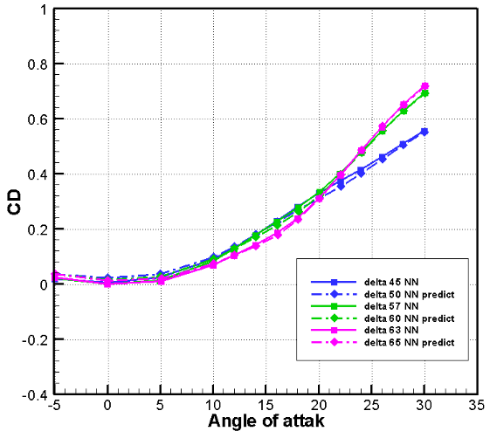

(b)Drag coefficient prediction for 50°, 60° and 65°

Fig. 12. Comparison of different sweep delta wing lift and drag coefficient result

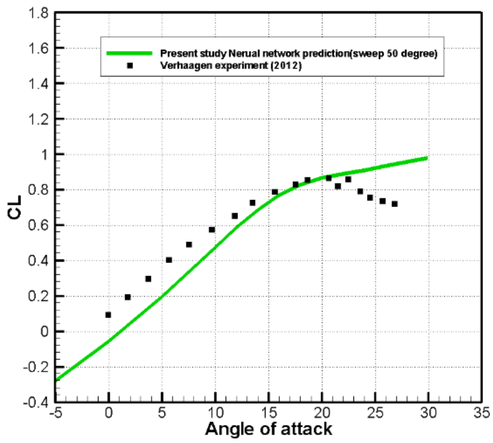

Fig. 13. The Comparison of 50° sweep angle delta wing lift coefficient prediction result with the reference literature

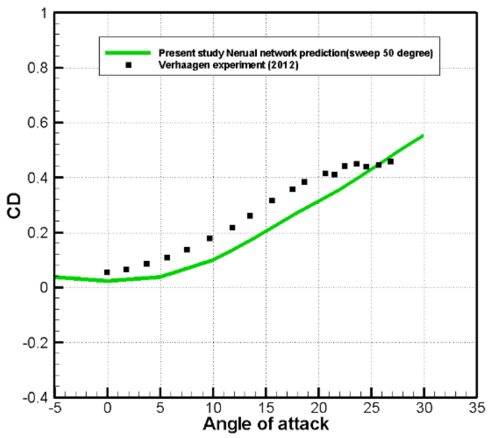

Fig. 14. The Comparison of 50° sweep angle delta wing drag coefficient prediction result with the reference literature

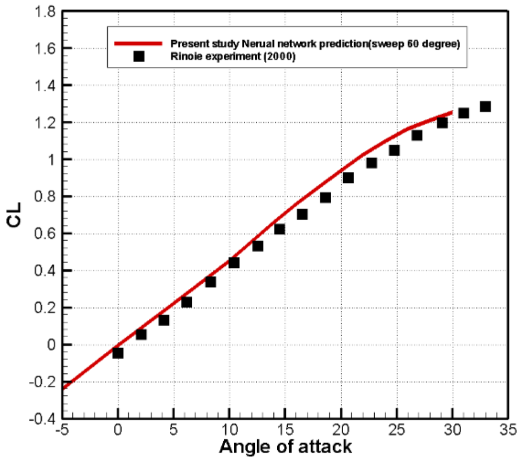

Fig. 15. The Comparison of 60° sweep angle delta wing lift coefficient prediction result with the reference literature

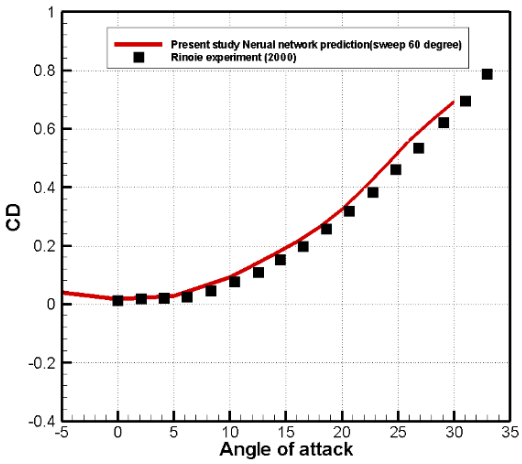

Fig. 16. The Comparison of 60° sweep angle delta wing drag coefficient prediction result with the reference literature

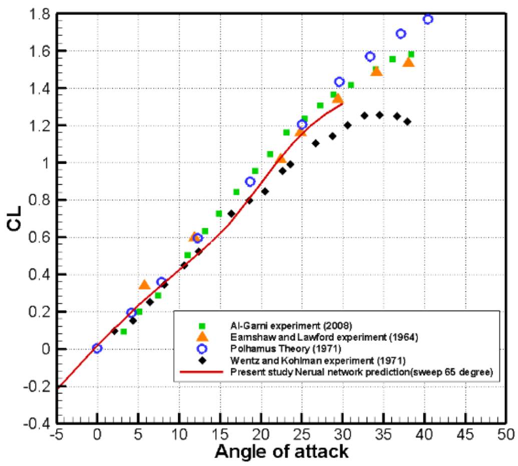

Fig. 17. The Comparsion of 65° sweep angle delta wing lift coefficient prediction result with the reference literature

CONCLUSIONS

In this study, we conducted the transient pressure measurement for cavity flow in transonic wind tunnel and lift and drag coefficient measurement for different sweep angle of delta wing in subsonic wind tunnel. The backpropagation neural network is used to train and verify the experiment result, where the Levenberg-Marquardt algorithm is adopted as the weight update method and the training results are well consistent with the experiment result.

For cavity flow case, the dynamic pressure data obtained in this study is then converted into spectral results for modal analyze. It is shown that the SPL of peak frequencies in the cavity of L/D=6 are larger than 150dB, which is caused by the strong oscillations of the compressible flow in the cavity. Qualitatively, both the training results and the experimental results are consistent with the existing semi-empirical formula.

From the subsonic delta wing test, it is found that the sweep angles of 57° and 63° have higher stall angle than sweep angle 45°, and the vortex breakdown phenomena is also observed from the flow field visualization results. By using neural network method, the prediction data of different sweep angle of delta wing can provide reasonable and useful results for application.

This study has completed the establishment of the neural network model for aerodynamics prediction. By the procedure of training and verification, neural network model can successfully predict the local transient pressure changes of the cavity flow case under different Mach numbers in transonic region and the lift/drag coefficient prediction in delta wing case in subsonic region. The result can reduce the pre-work time for wind tunnel testing and the prediction results can provide a reasonable aerodynamic information.

ACKNOWLEDGEMENT

Present work is supported by Department of Aerodynamics, Aeronautical Systems Research Division, National Chung-Shan Institute of Science and Technology and Department of Mechanical Engineering, National Chung-Hsing University.

REFERENCES

Al-Garni, A. Z., Saeed, F. and Al-Garni, A, M., “Experimental and Numerical Investigation of 65 Degree Delta and 65/40 Degree Double-Delta Wings”, Journal of Aircraft, Vol.45, No.1, January, pp.71-76. (2008).

Cigizoglu, H. K. and Kisi Ö., “Flow prediction by three back propagation techniques using k-fold partitioning of neural network training data”, Nordic Hydrology, Vol. 36, No. 1, pp 49-64 (2005).

Earnshaw, P. B. and Lawford, J. A., "Low-Speed Wind Tunnel Experiments on a Series of Sharp-Edged Delta Wings", Aeronautical Research Council Rept. and Memorandum No. 3424 (1964)

Efe, M.Ö., Debiasi, M., Yan,P., Özbay, H. and Samimy, M., "Neural Network Based Modeling of Subsonic Cavity Flows", International Journal of Systems Science, v.39, n.2, pp.105-117 (2008).

Faller, W. E., Schreck, S. J. and Luttges, M. W., "Real-Time Prediction and Control of Three-Dimensional Unsteady Separated Flow Fields Using Neural Networks", 32nd Aerospace Sciences Meeting & Exhibit (1994).

Gudmundsson, S., "General Aviation Aircraft Design Applied Methods and Procedures", Butterworth-Heinemann, 1st Edition, Appendix C1, pp.39-43 (2013).

Hagan, M.T. and Menhaj, M.B., "Training Feed-forward Networks with the Marquardt Algorithm", IEEE Trans. on Neural Networks, Vol.5, No. 6, pp. 989-993 (1994).

Heller, H. H., Holmes, D. G. and Covert, E. E., "Flow-induced pressure oscillations in shallow cavities", Journal of sound and vibration, Vol. 18, Issue 4, pp.545-553 (1971).

Hoyos, J. D., Suárez, G. and Echavarria, C., "Neural Network for Propeller Performance Prediction and CFD Validation of its Optimal", Journal of Aeronautics, Astronautics and Aviation, Vol. 54, No. 4, pp. 367-374 (2022).

Jarrah, M. A., and Ashley, H., "Impact of flow unsteadiness on maneuvers and loads of agile aircraft," 30th Structures, Structural Dynamics and Materials Conference (1989).

Khan, M. Z. A., Aziz, M. and Wijayanta, A. T., "Prediction of heat transfer enhancement of delta-wing tape inserts using artificial neural network", Vol. 27, Case Studies in Thermal Engineering, (2021).

Krishnamuty, K., "Acoustic radiation from two-dimensional rectangular cutout in aerodynamic surfaces", NACA-TN-3487 (1955).

McCulloch, W. and Pitts, W., "A logical Calculus of the Ideas Immanent in Nervous Activity", Bulletin of Mathematical Biophysics", Vol. 5, pp.115-133 (1943).

Polhamus, E.C., "Charts for Predicting the Subsonic Vortex-Lift Characteristics of Arrow", Delta and Diamond Wings", NASA TN D-6243, April. (1971).

Rinoie, K., "Experiments on a 60-Degree Delta Wing with Rounded Leading-Edge Vortex Flaps", Journal of Aircraft, Vol.37, No.1, pp.37-44 (2000).

Rosenblatt, F., "The perceptron: A Probabilistic Model for Information Storage and Organization in the Brain", Psych. Rev. 65, pp.386-408 (1958).

Rossiter, J. E., "Wind-tunnel Experiment on the Flow over Rectangular Cavities at Subsonic and Transonic Speeds", R. & M. No. 3438, British Aeronautical Research Council, Oct (1964).

Rumelhart, D. E., Hinton, G. E. and William, R. J., "Parallel Distributed Processing Explorations in the Microstructure of Cognition", Mit Press Computational Models of Cognition and Perception Series, Vol. 1, pp.318-362 (1986).

Seraj, S. and Martins, J. R. R. A., "Predicting the High Angle of Attack Characteristics of a Delta Wing at Low Speed", Journal of Aircraft Vol. 59, No. 4. pp. 1071–1081 (2022)

Tabaza, T. A., Tabaza, O., Barrett, J. and Alsakarneh, A., "Hysteresis modeling of impact dynamics using artificial neural network", Journal of Mechanics, Vol. 37, pp.333–338 (2021).

Tracy, M.B. and Plentovich, E. B., "Characterization of Cavity Flow Fields Using Pressure Data Obtained in the Langley 0.3-Meter Transonic Cryogenic Tunnel", NASA Technical Memorandum 4436 (1993).

Verhaagen, N. G. "Leading-Edge Radius Effects on Aerodynamic Characteristics of 50-Degree Delta Wings", Journal of Aircraft, Vol.49, No.2, March, pp.521-531. (2012).

Wentz, W. H. and Kohlman, D. L., "Vortex BREAKDOWN ON SLENDER SHARP-EDGED WINGS", Journal of Aircraft, Vol.8, No.3, March, pp.156-161. (1971).

Yanis, M., Arie, Y. B., Aneka, F. and Nova, Y., "Estimation of Surface Roughness Value Using Back Propagation Neural Network on Green Machining", Journal of Mechanical Engineering Research and Developments, Vol. 44, No. 8, pp. 241-249 (2021).

應用倒傳遞類神經網路預測氣動力試驗數據研究

歐陽駿塏　廖翊廷　李穎　王威翔
國家中山科學研究院航空研究所
國立中興大學機械工程學系

摘 要

本研究目的在建立倒傳遞類神經網路模型來分別預測穿音速風洞與次音速風洞試驗的氣動力數據，穿音速風洞以戰機內置彈艙外型簡化為簡單凹槽幾何之概念進行可壓縮流凹槽壓力量測試驗，

並獲得動態壓力變化試驗數據，次音速風洞以不同後掠角角度的三角翼進行試驗，利用內置式力平衡儀量測模型的升力係數與阻力係數。分別將穿音速風洞與次音速風洞試驗結果作為類神經網路模型的訓練參數，因類神經網路訓練結果會因為不同的隱藏層/神經元數量而影響學習速率與正確率，本研究利用試誤法進行參數調整並決定所需神經網路架構，並以 Levenberg-Marquardt 演算法作為權重更新的方法以最小化誤差函數，本研究已完成倒傳遞類神經網路模型建立，經驗證後可應用於預測穿音速風洞凹槽模型特定位置於不同馬赫數條件之壓力變化，及藉由改變三角翼外型幾何參數預測次音速風洞不同後掠角角度的三角翼升力係數與阻力係數，所獲得結果比較試驗結果均具有一致性，利用類神經網路方法可減少風洞試驗前準備的前置作業時間，預測結果可作為氣動力數據分析的參考資訊。